Journal of Sol-Gel Science and Technology, **2015**, *75*, 215-223.

The effect of sol-gel preparation conditions on structural characteristics and magnetic properties of M-type barium hexaferrite thin films

E.D. Solovyova[1*], M.L. Calzada[2], A.G. Belous[1]

[1]Department of Solid State Chemistry, V.I. Vernadskii Institute of General and Inorganic Chemistry, 32/34 Prospect Palladina, Kyiv-142, 03680, Ukraine

Phone /Fax : +380 44 424 22 11

E-mail: solovyovak@mail.ru, belous@ionc.kiev.ua

[2]Department of Ferroelectric Materials-ICMM, Institute of Materials Science, C/ Sor Juana Inés de la Cruz, 3, CSIC, Cantoblanco, 28049 Madrid, Spain

Phone /Fax : +34 91 334 90 62

E-mail: lcalzada@icmm.csic.es

*author to whom correspondence should be addressed.

V.I.Vernadskii Institute of General and Inorganic Chemistry, 32/34 Prospect Palladina, Kyiv-142, 03680, Ukraine

Phone /Fax : +380 44 424 22 11, E-mail: solovyovak@mail.ru

Abstract

We have shown the possibility to obtain M-type barium hexaferrite thin films with thickness of ~ on the surface of dielectric α-Al_2O_3 substrates with low microwave dielectric loss (tan δ ~ 10^{-4} GHz) by a sol-gel method. For the production of high-dense homogeneous thin films of M-type barium hexaferrite ($BaFe_{12}O_{19}$, BHF) with nanorod-like grains and a uniform distribution of iron and barium ions, we have studied the synthesis conditions for thermally stable film-forming solutions with high concentrations of barium ions. Films with a c-axis magnetic texture were obtained by spin coating the former solutions on α-Al_2O_3 substrates and annealing at temperatures between 473K and 1073K. The resulting textured M-type BHF films have demonstrated the following magnetic parameters: Hc⊥ = 334 kA/m, $H_{c||}$ = 167 kA/m; $M_{s\perp}$ = 0.005 emu, $M_{s||}$ = 0.003 emu (for the films' thickness of ~200 nm), and $H_{c\perp}$ = 360 kA/m, $H_{c||}$ = 338 kA/m; $M_{s\perp}$ = 0.009 emu, $M_{s||}$ = 0.007 emu for the films' thinkness of ~ 450 nm. These M-type BHF thin films can serve as a promising basis for further development of multilayer microwave resonant elements.

Keywords: barium hexaferrite, sol-gel synthesis, non-crystalline thin films, c-axis magnetic texture, magnetic characteristics, surface microstructure.

1. Introduction

M-type barium hexaferrite ($BaFe_{12}O_{19}$) (hereinafter BHF) is characterized by high values of coercivity (H_c) and saturation magnetization (M_s) due to a strong uniaxial magnetocrystalline anisotropy along hexagonal *c*-axis [1]. The prospective applications of M-type BHF are governed by a combination of unique magnetic properties and its chemical stability, corrosion resistance and cheapness of the initial components. The synthesis of nanocrystalline thin films is important for different technical applications [2-7]. The interest in nanocrystalline films of M-type BHF is due to their potential applications in high-density low noise recording media, storage systems [8], and microwave (MW) devices [9 - 14]. Moreover, in the latter case, a film can be used either alone [12-14] or as a component of multilayer MW resonant elements with the properties controlled by an external magnetic field [4, 12, 15]. For the applications in high-density low-noise recording systems, thin films (thickness of ≤ 1 μm) are generally produced. For them, monocrystalline silicon is often used as a substrate [16-19]. For the applications in microwave devices, both thin and thick films (thickness > 1 μm) deposited on high-Q microwave dielectric substrates (a dielectric with low dielectric loss tan δ in the MW range) are required. For instance, thick films of the M-type BHF on the surface of high-Q dielectric α-Al_2O_3 substrates have been reported elsewhere [12]. However, the deposition of both M - type BHF thick and thin films high-Q dielectric substrates is required for the development of multilayer microwave resonant elements.

Deposition methods, such as sputtering [20-21], pulsed laser deposition [22-23] and electron beam evaporation [24], are the most used for the preparation of such thin films. However, these methods often lead to the formation of not enough dense and homogeneous films [25], and, in addition, they require very expensive equipment. To date, one of the most promising methods for production of M-type BHF polycrystalline thin films is chemical solution deposition (CSD) [16, 25-27]. This includes the synthesis of the precursor solution by sol-gel chemistry, which makes possible the preparation of high-dense and homogeneous nanocrystalline thin films without using

expensive equipment. At the same time, the annealing temperatures of the films is, in general, much less in comparison with other methods. This contributes to a reduction of the particle size of the material and, consequently, improves the films characteristics. A huge number of works have reported on sol-gel M-type BHF thin films deposited on silicon substrates [16-19]. However, the data on BHF thin films on the surface of α-Al_2O_3 is limited. We have studied here the possibility to produce homogeneous and high-dense BHF thin films with a controllable thickness, on the surface of high-Q dielectric α-Al_2O_3 by CSD.

Sol-gel synthesis of high-dense homogeneous nanocrystalline films depends on many factors, such as wetting of the substrate by the film forming solutions (FFS) (wetting angle and gel viscosity), film deposition rate (for spin-coating process – substrate rotation speed), heat treatment conditions, etc.

In the synthesis of uniform films, a key point is to maintain the homogeneity of the initial sol-gel system during removing of solvent from the deposited solution layer. The possibility of homogeneity violation of the system at heat treatment of the FFS (at T = 353 - 523K) can be significant during the sol-gel synthesis of BHF. This may be attributed to a lower stability of chelate complexes of Ba^{2+} ions as compared to such complexes of Fe^{3+} ion [28]. This results in the formation of undesirable secondary phases with the increase of the crystallization temperature of BHF. This problem can be solved by increasing the gels thermal stability by increasing the gel viscosity [29]. On the other side, the initial concentration of barium ions, as a rule, is limited in the range 0.05- 0.08 mol/L [30,31]. At such low metal ion concentration, the deposition of large number of layers is required to reach the desired film thickness. This significantly reduces the productivity and increases the energy and labor costs. Therefore, the investigation of the synthesis conditions of thermally stable film forming solutions (FFS) with higher barium ions concentrations is important.

The aim of this work is the study of the synthesis conditions for getting thermally stable film-forming solutions (FFS) with high concentrations of barium ions. These solutions will be used

in the production of homogeneous and high-dense M-type BHF thin films on high-Q dielectric α-Al_2O_3 substrates. The heat treatment conditions for the crystallization of the M-type BHF thin films, their structural features and magnetic properties have also been studied.

2. Experimental methods

2.1. Synthesis and characterization of sol-gel precursors for BHF thin films preparation.

Analytically pure $Ba(NO_3)_2$, $Fe(NO_3)_3 \cdot 9H_2O$, citric acid (CA), ethylene glycol (EG), and 25% aqueous ammonia were used for the preparation of the film forming solutions (FFS). The iron and barium nitrates were dissolved in distilled water (molar ratio Fe/Ba = 12). The concentration of barium ions was 0.08, 0.16, 0.24 and 0.30 mol/L. The molar ratio of citric acid and total metal cations (CA/M) was 1.5. After solution homogenization (at 360 – 370 K with stirring for 5 min), ethylene glycol was added. The citric acid/ethylene glycol (CA/EG) molar ratio was 1/3 (for solution with barium ion concentration of 0.08 mol/L) and 1/5 (for solution with barium ion concentration of 0.08, 0.16, 0.24 and 0.30 mol/L). The solution pH was adjusted to 8 with 25% aqueous ammonia under continuous stirring. The FFS was heated at 353K (for 15, 30, 45, 60 75 and 90 min) under stirring to obtain the desired viscosity.

The viscosity of the FFS was measured by glass capillary viscometer with a capillary diameter of 0.62 mm. The kinematic viscosity of FFS was calculated from the formula: $V = \frac{g}{980,7}\tau \times 0,01187$, where V – the kinematic viscosity, cSt ; g – acceleration due to gravity at the measurement site, cm/s^2; τ – time to expiration of the liquid, s.

The wetting angle θ was defined by the method of spreading droplets [32] from the condition of mechanical equilibrium of three-phase contact line (solid, liquid and phase – "precursor", which contacted with a solid surface before a liquid supply) on the main liquid droplet size applied to hard surfaces. Values of cosθ were calculated by the formula:

$$\cos\theta = (\frac{d}{2})^2 - h^2 \Big/ (\frac{d}{2})^2 + h^2$$

where *h* is the height and *d* the diameter of the droplet base. Parameters of drop, *h* and *d*, were measured using the apparatus which are the basic units of cathetometer measuring cell - cell and a lighting device, providing a contrast image of the drop and the surface under study.

Thermogravimetric and differential thermal analysis (TGA/DTA) were carried out on BHF powders obtained from the film-forming solutions after drying overnight at 373K. The experiments were carried out in dynamic air or oxygen atmospheres, 100 mL/min, from room temperature to 1173K, using a Seiko TGA/DTA equipment.

IR spectra of the air-dried and calcined (T = 573, 723, 573, 873 and 1073 K for 1 hour) sol - gel powders were recorded on Specord-M3l spectrometer in the range 200 - 4000 cm^{-1}. The tablets-like test samples were prepared with KBr.

2.2. Preparation and characterization of nanocrystalline sol-gel films of M-type BHF.

The film forming solutions were spin-coated at 3600 rpm for 20s on α-Al_2O_3 substrates, with low microwave dielectric loss (tan $\delta \sim 10^{-4}$ GHz). Each layer was dried at T = 473K and T = 683 – 673 K.

For the annealing of the thin films, high and slow heating rates were used. The slow heating annealing was carried out in a conventional furnace at a heating rate of 278K/min. Temperatures and soaking times were of 473K/20 min, 723K/30 min and 973-1073K/60 min.

The rapid annealing (rapid thermal processing, RTP) was carried out in a furnace with infrared heating, using a heating rate of 180 °C/min. Temperatures and soaking times here were of 623K/10 min and 973/20 min.

Thin films were characterized by X-ray diffraction analysis (XRD) on a D8-Bruker X-ray powder diffractometer with CuKa radiation and Bragg-Brentano geometry. For the phase characterization, the JCPDS database was used.

The surface micrographs of the films were obtained using a field emission gun scanning electron microscope (FEG-SEM, Nova Nanosem 230 FEI Company equipment, Hillsboro, OR).

Magnetic characterization of the films was carried out in a vibrating sample magnetometer (VSM; MLVSM9 MagLab 9 T, Oxford Instrument). Samples were placed parallel and perpendicular to the magnetic field and the magnetization curves were recorded at 295K by subjecting the sample to a field of ± 5 T at 0.5 T/min.

3. Results and discussion

Table.1 shows the effects of the solution processing conditions and barium ion concentration (mol/L) on the viscosity of the sol-gel systems (η, cSt). Viscosity increases with increasing time of heating of the solution and with the ethylene glycol and barium concentrations. Stability of the solutions is increased with viscosity.

During the deposition on α-Al_2O_3 substrates of the film formation solutions (FFS) with concentration of barium ions equal to 0.08 mol/L and different times of heating of the solution (samples FFS-1 and FFS-2, Table 1), it has been determined that the best adhesion is observed for solutions with CA/EG = 1/5 and a viscosity in the range of 3.30 - 3.85 cSt. Using these solutions, nanocrystalline M-type BHF films with different number of layers (from 4 to 10) were prepared. However, BHF crystalline phase were not detected by XRD even on 10 layers films after heat treatment at T= 1073 - 1273K. This is explained by the low concentration of initial metal ions and BHF yield.

Therefore, FFS with barium ions concentration equal to 0.16, 0.24 and 0.30 mol/L (CA/ EG = 1/5) were used for the preparation of BHF films. As follows from Table 1, the viscosity of the FFS depends on the time of heating of the solution (45 - 75 min.); it is in the range from 3.67 to 5.32 cSt. During deposition of these solutions on the substrate, it has been shown that the precursors with 0.3 mol/L barium ions concentration (sample FFS-5) are characterized by a good adhesion to the substrate. The wetting angles for the FFS-5 sample after times of solution heating of 45, 60 and 75 min (η = 4.02, 4.53 and 5.32 cSt respectively) were determined (Fig. 1). The smallest angle, and accordingly, the best adhesion to the substrate surface is observed for FFS-5, with η = 4.02 cSt

obtained with a time of heating of 45 min. Therefore, this FFS-5 solution (η = 4.02 cSt, barium ions concentration equal to 0.3 mol/L) was used for the deposition of BHF thin films.

Thermal decomposition analysis and IR spectra of the sol-gel powders were studied for defining the temperature range of elimination of the organic compounds and, therefore, the prebaking temperatures of the films that have to be used. Figure 2 shows the (TG – DTA) curves of the sol-gel powders calcined at T = 473K, and Figure 3 shows the IR spectra of the powders calcined at T = 473K, 723K, 773K, 873K and 1073K. As follows from Figure 2, the DTA curve is characterized by a major exothermic process with a máximum at a temperature of T = 640K. The mass loss of the sample at low temperatures ($T \leq 573K$) primarily is due to removal of adsorbed (H_2O molecules) and structural (OH - groups) water. The thermal decomposition of barium and iron nitrates also occurs in this temperature range. According to [33], the decomposition of ferric nitrate in the presence of citric acid can lead to the formation of γ-Fe_2O_3. The diffraction patterns of these samples confirm this fact (Figure 4). As follows from Figure 4, the α-Fe_2O_3 phase is observed on the XRD patterns of samples after a heat treatment at 623K. The mass loss of the sample in the temperature range of T = 573-773K is produced by the citric acid decomposition. Further increasing of temperature causes the formation of barium hexaferrite phase (Figure 4) which is accompanied by a decomposition of the residual organic components.

The analysis of the IR spectra (Figure 3) shows that the initial sample (T = 523K) is characterized by low intensity stretching M-O vibrations (in the range 310 - 582 cm^{-1}), CO_3^{2-} and HCO_3^{3-} - ions vibration (in the range 1380-1610 cm^{-1}). The enhancement of the intensity of the CO_3^{2-}- groups vibrations in the IR - spectra of powders calcined at T = 723K points to the degradation of organic components at these conditions. The low intensity of these vibration on the spectra of the samples calcined at T = 873 K and 1073 K, indicates the decomposition of barium carbonate at T > 723K. These results are consistent with TG - curve of the samples of Fig. 2. Based on them, the temperature range for the pre-heat treatment of the films was established at T = 673 – 723K.

The investigation of the microstructure of the thin films (4 layers) shows that it is characterized by a thickness of ~200 nm (Fig. 5,a) and nanorod-like grains ($d_{av.}$, $l_{av.}$ = 60 nm, 320 nm) (Fig. 5,b). According to the EDX-analysis, the films have a uniform distribution of barium and iron ions on ~~its~~ their surface (Fig.6). These results indirectly confirm the preservation of the homogeneity, not only at removing the solvent, but also at all stages of the films preparation.

Figure 7 shows the XRD patterns of the BHF films (4 layers) obtained under different treatments: with a low heating rate at T = 1073 K and 1173K (patterns 1 and 2) and with a rapid heating rate at T = 973K and 1173K (patterns 3 and 4). All samples are hexaferrite single-phase. The XRD patterns 3 and 4 (rapid heating rate) differ from the the patterns 1 and 2 (low heating rate). A significant increase of the 006 and 008 reflexions is observed. This indicates the preferential orientation of grains along the [00l] direction. An axis of easy magnetization of BHF is directed along the hexagonal *c*-axis, therefore such grains orientation may indicates the appearence of an axial magnetic texture in these these films. A similar structure has been reported by other authors [31]. A texture degree of 40 and 50% is calculated for the films obtained after the thermal treatments at T = 973K and 1173K. The degree of texture was determined by the formula [34]:

$$f = \frac{p - p_0}{1 - p_0} \times 100\%,$$

where p_0 and p - the ratio of the sum of 00l reflections intensities to the sum of intensities of all (00l + hkl) reflections on diffractograms of non-textured and textured BHF films respectively. The films texture can be affected by many factors, such as processing conditions or substrate nature [35-41]. As follows from Fig. 7, the formation of BHF textured films occurs only here with a rapid heating. This can be explained by the fact that, with a low heating film crystallization starts during the heating process, and, as the temperature increases, more energy is available to surmount the barriers for nucleation events in addition to the energetically most favorable nucleation event [35]. Such conditions are favorable for the spontaneous growth of nucleus (a homogeneous nucleation mechanism). In this case, texture is not observed in these films. With a rapid heating, a directional

heat flow is produced and leads to the formation of a temperature gradient on the film–substrate interface. In this case, we observe a heterogeneous nucleation mechanism which promots epitaxial orientation of the BHF grains at the film–substrate interface [35, 37, 40-41]. The α-Al_2O_3 substrate has a rhombohedral structure (R3C space group), which accurs the hexagonal syngony [42]. Relative mismatches of crystalline lattice parameters (ε) of both the substrate and hexagonal BHF (sp. gr. $R6_3/mmc$) film at the interface were determined by the formula [43]:

$$\varepsilon = \frac{a_f - a_s}{a_f},$$

where a_f and a_s – crystalline lattice parameters of an epitaxial solid solution (M type BHF) and substrate (α-Al_2O_3), respectively. The relative mismatches of crystalline lattice parameters (ε) for ***a*** and ***c*** parameters are: 0.24 and 0.78, respectively. Obviously, the grains of films grow perpendicular to the *c* - axis with a such difference in these mismatch parameters. Therefore, for films deposited on the α-Al_2O_3 substrate, the grains orientates along the [00l] direction. This leads to high reflections from the (008) crystal plane and those planes closed to (008) (Fig. 7, diffractogramms 3 and 4).

According to Ref. [44-46], the change in the film thickness can lead to changes in structure, which causes changes in the film properties. In this regard, we have synthesized 4-layers deposited films with an average thickness of ~200 nm, and 10-layers deposited films with an average thickness of ~450 nm, both with nanorod-like grains ($d_{av.}$, $l_{av.}$ = 40 nm, 205 nm) (Figure 8). Fig. 9 shows the diffraction patterns of the 4 and 10-layers films after their heat treatment at 973K. As follows from Figure 9, the film texture degree decreases with increasing the films thickness. This indicates that the film is more textured at the film - substrate interface, and part of film texturing decreases with increasing the film thickness [35]. These results are consistent with the magnetic measurements results of the films (Fig. 10). As can be seen, the anisotropy of the film magnetic properties decreases with increasing the film thickness (Fig. 10,a,b). For 4-layers films, the

difference between coercivity measured perpendicularly and parallel ($H_{c\perp}$- $H_{c\parallel}$) to the film plane is 167 kA/m, and for 10-layers film – 23kA/m.

Comparing the films prepared in this work and and those of ref. [12, 16-18, 20-25], we can note that the films obtained by tape-casting in ref. [12] are characterized by more larger grains sizes. Usually, a density of coarse-grained films is lower than a density of fine-grained films. In particular, auhors [12] indicates that films are weakly textured and contain pores. Films obtained in [20 - 25] by physical deposition methods are also characterized by a large grain size and pores. Furthermore, these films have lower magnetic properties (Ms, Hc) in comparison with the films of this study. Films synthesized on the silicon substrates [16-18] are multiphase, weakly textured and pores are observed at the surface.

High-density textured thin films with fine grains and high magnetic characteristics have been produced in this study. Therefore, these M-type BHF films of are promising for the further development of multilayer microwave resonant elements "high-Q dielectric – M-type BHF thin film".

4. Conclusion

The possibility of preparing M-type barium hexaferrite (BHF) thin films on the surface of dielectric α-Al_2O_3 substrates by a sol-gel method has been shown. The conditions for the synthesis of thermally stable film-forming solutions with an increased concentration of barium ions (0.3 mol/L), and the viscosity of η = 4,02 cSt –used further for the productions of M-type BHF thin films- have been studied. The temperature range for the pre-heating of the films has been defined in the T = 673 – 723K range. Thin nanocrystalline films of M-type BHF with thickness of 200 and 450 nm, and nanorod-like grains ($d_{av.}$, l_{av} = 60 nm, 320 nm and d_{av}, l_{av} = 40 nm, 205 nm, respectively) have been prepared. A uniform distribution of iron and barium ions over the substrate's surface is proved. The BHF thin films have been shown to exhibit the *c*- axis magnetic texture after a rapid heating for their crystallization. The texture degree of these BHF thin films decreases with increasing film thickness ($H_{c\perp}$- $H_{c\parallel}$ = 167 kA/m and 23 kA/m for the film thickness 200 and 450

nm, respectively). These textured films of M-type BHF are promising for the future development of multilayer microwave resonant elements.

Acknowledgements

We acknowledge the project "Nanolicom" (FP7-PEOPLE-2009-IRSES program, 2011-2014, Grant agreement № 247579) and the partial support of the Spanish Project MAT2013-40489-P.

References

1. Smith J, Wijn HPJ (1959) Ferrites. Philips Technical Library, Eindhoven.

2. Marc J. de Vries (2005) 80 years of reaserch of the Philips natuurcunding laboratorium. Pallas Publications, Amsterdam.

3. Moulson AJ, Herbert JM (2003) Electroceramics. Second edition: Materials, properties, application. Wiley, New York.

4. Koledintseva MY, Khanamirov AE, Kitaitsev AA (2011) Advances in Ceramics – Electric and Magnetic Ceramics, Bioceramics, Ceramics and Environment. InTech: 550-527.

5. Pfeiffer H, Chantrell RW, Görnert P J (2000) Magn Magn Mater 125: 373–376.

6. Mikhailovsky LK, Pollak BP, Khanamirov AE (2002) Research and development of BHF hexaferrite devices in MPEI. Proc. 9th Int. Conf. on Spin Electronics, Moscow: 559–573.

7. Meshram MR, Agarwal NK, Sinha B, Misra PS (2004) J Magn Magn Mater 271: 207–213.

8. Hylton TL, Ulllah MA, Coffey KR, Umphress R, Howard JK (1994) J Appl Phys 75 (10): 5960-5965.

9. Lei F, Xiaogang L, Zhang Y, Vinayak P (2003) Nano lett 3 (6): 757–760.

10. Harris VG, Chen Z, Chen Y, Yoon S, Sakai T, Gieler A, Yang A, He Y, Ziemer KS, Sun N X, Vittoria C (2006) J Appl Phys 99: 08M911–08M915.

11. Frey NA, Heindl R, Srinath S, Srikanth S, Dudney NJ (2005) Mat Res Bull 40: 1286–1293.

12. Harris VG (2012) IEEE Trans Magn 48 (3): 1075-1104.

13. Peng B, Wang Y, Zhang W, Zhang W, Tan K (2012) Mod Phys Let B 26: 1250168 -1250174.

14. Chen Y, Geiler AL, Sakai T, Yoon SD, Vittoria C et al. (2006) J Appl Phys 99: 08M904 (1-3).

15. Harris VG, Geiler A, Chen Y, Yoon SD, Wu M, Yang A, Chen Z, He P, Parimi PV, Zuo X, Patton CE, Abe M, Acher O, Vittoria C (2009) J Magn Magn Mater 321: 2035–2047.

16. Li H, Huang J, Li Q, Li Q, Su X (2009) J Sol-Gel Sci Techn 52: 309-314.

17. Pramanik NC, Fujii T, Nakanishi M (2005) Mater Let 59: 468– 472.

18. Santos JVA, Macedo MA, Cuhna F, Sasaki JM, Duque JGS (2003) J Microel 34: 565-567.

19. Masoudpanah SM, Seyyed Ebrahimi SA (2011) J Magn Magn Mater 323: 2643–2647.

20. Nakagawa S, Matsushita N., Naoe M (2001) J Magn Magn Mater 235: 337-341.

21. Chandrasekhar R, Mapps DJ (1996) J Magn Magn Mater 157-158: 326–328.

22. Lisfi A, Lodder JC (2002) J Magn Magn Mater 242–245: 391–394.

23. Lisfi A, Nguyen LT, Lodder JC, Williams CM, Corcoran H, Chang P, Johnson A, Morgan W (2005) J Magn Magn Mater 290-291: 219–222.

24. Wane I, Bassudou A, Cosset F, Ce´le´rier A, Girault C, Decossas JL, Vereille JC (2000) J Magn Magn Mater 211: 309-313

25. Zhang XY, Ong CK, Xu SY, Fang HC (1999) Appl. Surf. Sci. 143: 323-327.

26. Zhang W, Tang H, Peng B, Zhang W (2010) Appl Surf Sci 257: 176–179.

27. An SY, Lee SW, Shim IB, Kim CS (2002) Phys St Sol (a) 189: 893-896.

28. Lee W-J, Fung T-T (1995) J Mater Scien 30: 4349-4354.

29. Brinker CJ, George W (1990) Scherer Sol-gel Science: The Physics and Chemistry of Sol-gel Processing, Gulf Professional Publishing.

30. Qui J, Lan L (2006) Mat Scien Engin B 133: 191–194.

31. Li H, Huang J, Li Q, Xiaodong S (2009) J Sol-Gel Sci Tech 52: 309–314.

32. Yuan Y, Lee TR (2013) Contact Angle and Wetting Properties, Springer Series in Surf. Sci. 51: 3-34.

33. El-Sheikh SM, Harraz FA, Abdel-Halim KS (2008) Synthesis and Characterization of Mesoporous Iron Oxide by Solid Thermal Decomposition Reaction for Catalytic Oxidation of CO, International conference on nanotechnology and applications. 615-005: 132-137.

34. Lotgering FK (1959) J Inorg Nucl Chem 9: 113-123.

35. Ricote J, Poyato R, Alguero M, Pardo L, Calzada ML (2003) J Am Ceram Soc 86 (9): 1571–77.

36. Zhuang Z, Kryder MA, White RM, Laughlin DE (1999) C-axis perpendicularly oriented barium ferrite thin film media on silicon substrate, MRS Proceedings, 562: 605-610.

37. Liu L, Zuon R, Lian Q (2013) Ceram Intern 39: 3865–3871.

38. Jin ZQ, Liu JP (2006) J Phys D: Appl Phys 39: R227–R244.

39. Jiang SW, Zhang QY, Huang W, Jiang B, Zhang Y (2005) Appl Surf Sci 252 (24): 8756–8759.

40. Acharya BR, Prasad S, Venkataramani N, Shringi SN, Krishnan R (1996) J Appl Phys 478 (79): 478–484.

41. Suzuk Y (2001) Annu Rev Mater Res 31: 265–289.

42. Hahn Th (2005) International Tables for Crystallography A: Space Group Symmetry A, Springer, New York.

43. Ayers JE (2007) Heteroepitaxy of semiconductors: theory, growth, and characterization, Taylor & Francis Group, LLC.

44. Capraro S, Chatelon JP, Joisten H, Le Berre M, Bayard B, Barbier D, Rousseau JJ (2003) J Appl Phys 93: 9898–9901.

45. Park N-J, Field DP, Nowell MM, Besse PR (2005) J Electr Mater 34 (12): 1500–1508.

46. Kim DH, Nam IT, Hong YK (2003) Mater Sci -Wroclaw 21: 65–72.

Figure captions

Fig.1. Wetting angle of forming film solutions (FFS) on the α-Al_2O_3 substrate at different viscosity. a, b, c - samples with a viscosity÷ of 4.02, 4.53 and 5.32 cSt, respectively.

Fig.2. TG -DTA analyse of dried (T = 473K) BHF sol-gel powder samples.

Fig.3. IR spectra of BHF sol-gel powder samples (CA/EG = 1/5) obtained at different temperatures: 1, 2, 3 and 4 – T = 473, 723, 873 and 1073 K, respectively.

Fig.4. X-ray diffraction (XRD) patterns of powder samples obtained at different temperatures: 1 – 473K, 2 – 623K, 3 – 973K, 4 – 1073K, 5 – 1173K.

Fig.5. Cross-section (a) and surface (b) microstructures of the BHF film (4 layers) prepared at T = 1173K (SEM).

Fig.6. Distribution of iron and barium ions on the BHF film (4 layers) surface after heat treatment at T = 1173K (EDX).

Fig.7. X-ray diffraction (XRD) patterns of the BHF thin films (4 layers): 1 and 2 – slow heating rate (T = 1073 and 1173K respectively); 3 and 4 – rapid heating rate (T = 973 and 1073K respectively).

Fig.8. Cross-section (a) and surface (b) microstructures of the BHF film (10 layers) at T = 973K (SEM).

Fig.9. X-ray diffraction (XRD) patterns of the thin BHF films obtained by a rapid heating at T = 973K: 1 and 2 – 10 and 4 layers respectively.

Fig.10. Hysteresis loops of BHF 4-layers (a) and 10-layers (b) thin films obtained at 973K.

Table 1

The viscosity of the sol-gel systems at the different conditions of preparation

Film forming solution (FFS)	Citric acid/ ethylene glycol (CA/EG)	Barium ions concentration, mol/L	The viscosity of the sol-gel system η, cSt						The stability of gel (number of days)
			The time of heat treatment of the sol-gel system at T = 353K t, min.						
			15	30	45	60	75	90	
1	1/3	0.08	2.67	2.97	3.12	3.29	3.45	3.63	10
2	1/5	0.08	2.87	3.07	3.30	3.56	3.72	3.85	12
3	1/5	0.16			3.67	3.96	4.32		20
4	1/5	0.24			3.72	4.26	4.82		20
5	1/5	0.30			4.02	4.53	5.32		25

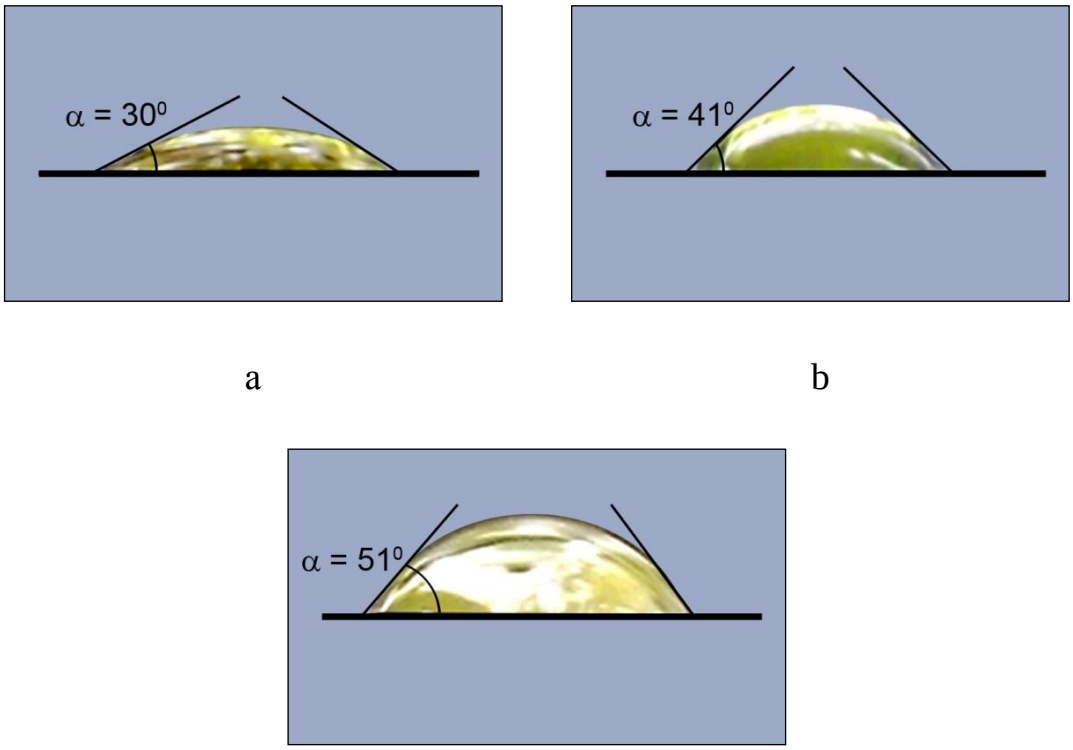

Figure 1

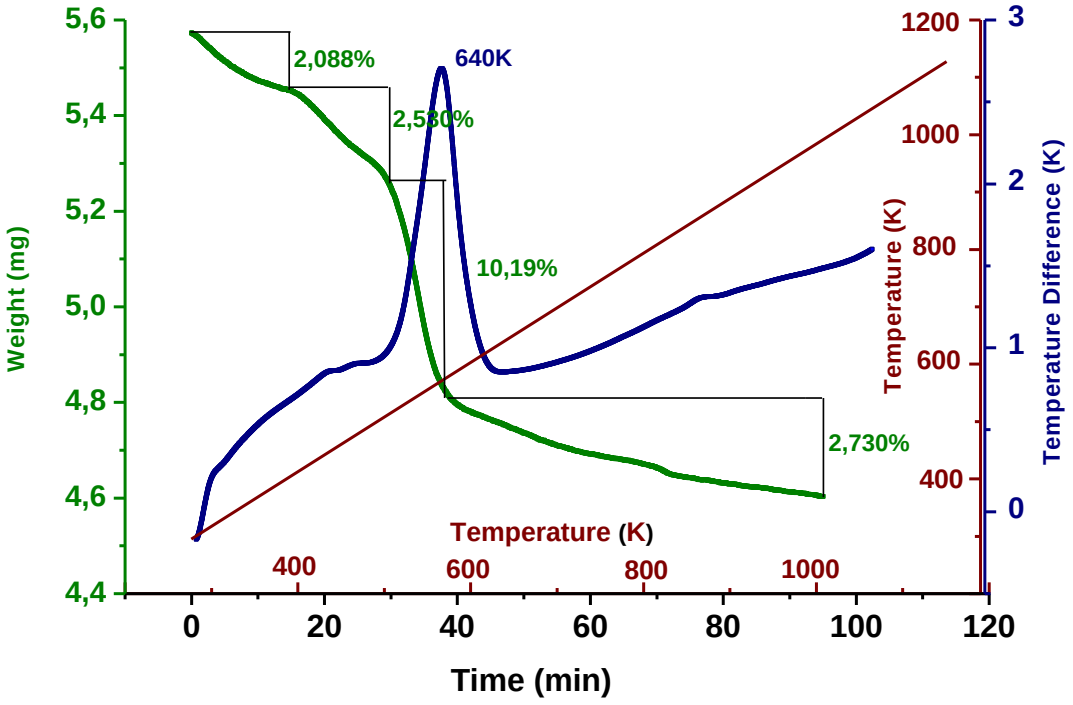
Weight (mg)
5,6
5,4
5,2
5,0
4,8
4,6
4,4
2,088%
640K
2,530%
10,19%
2,730%
Temperature (K)
400
600
800
1000
1200
Temperature Difference (K)
3
2
1
0
Temperature (K)
0
20
40
60
80
100
120
Time (min)

Figure 2

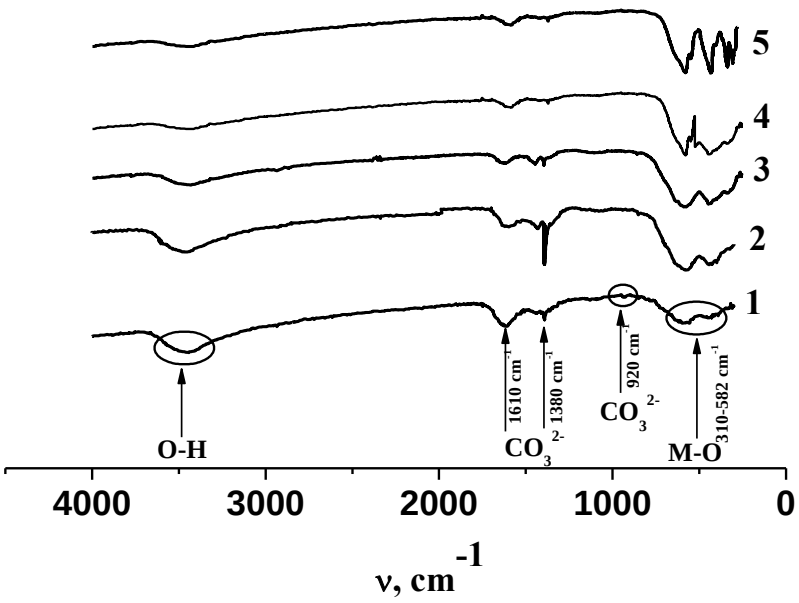
5
4
3
2
1
O-H
1610 cm-1
CO3 2-
1380 cm-1
920 cm-1
CO3 2-
M-O
310-582 cm-1
4000
3000
2000
1000
0
ν, cm-1

Figure 3

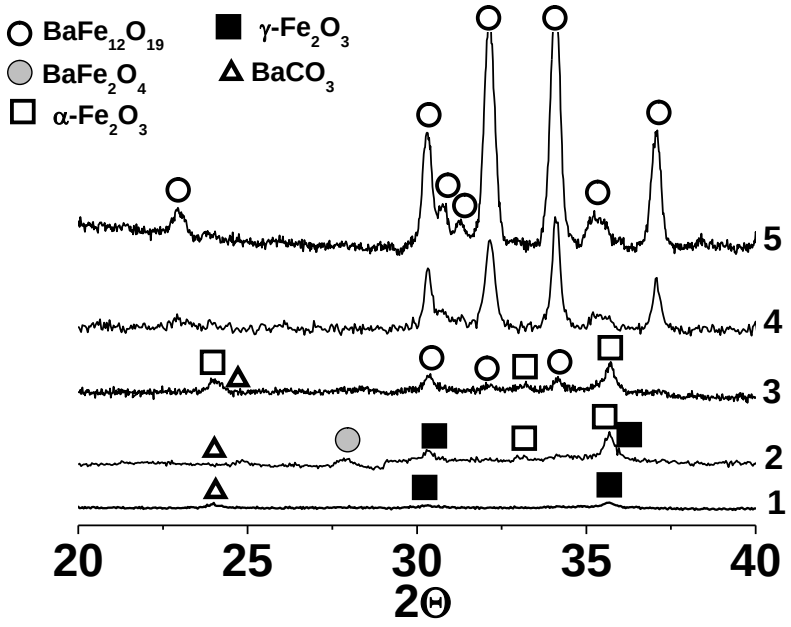
BaFe12O19
γ-Fe2O3
BaFe2O4
BaCO3
α-Fe2O3
5
4
3
2
1
20
25
30
35
40
2Θ

Figure 4

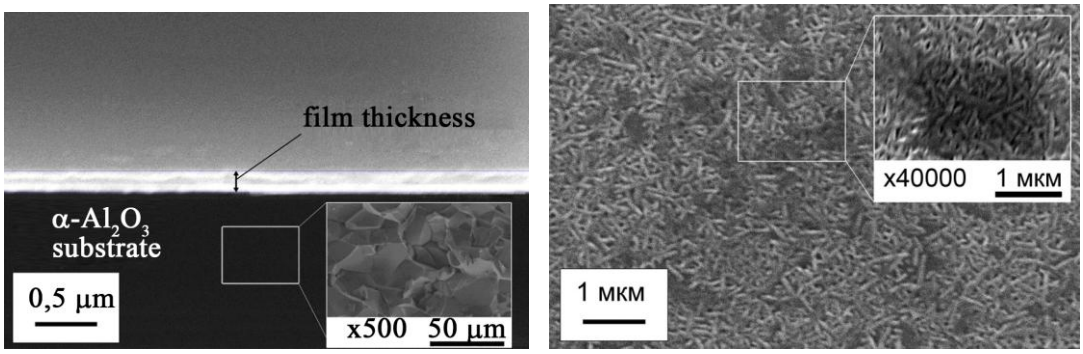
film thickness
α-Al2O3
substrate
0,5 μm
x500 50 μm
x40000 1 мкм
1 мкм

a b

Figure 5

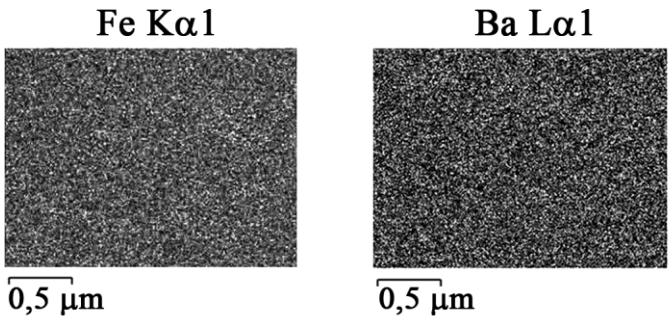

a b

Figure 6

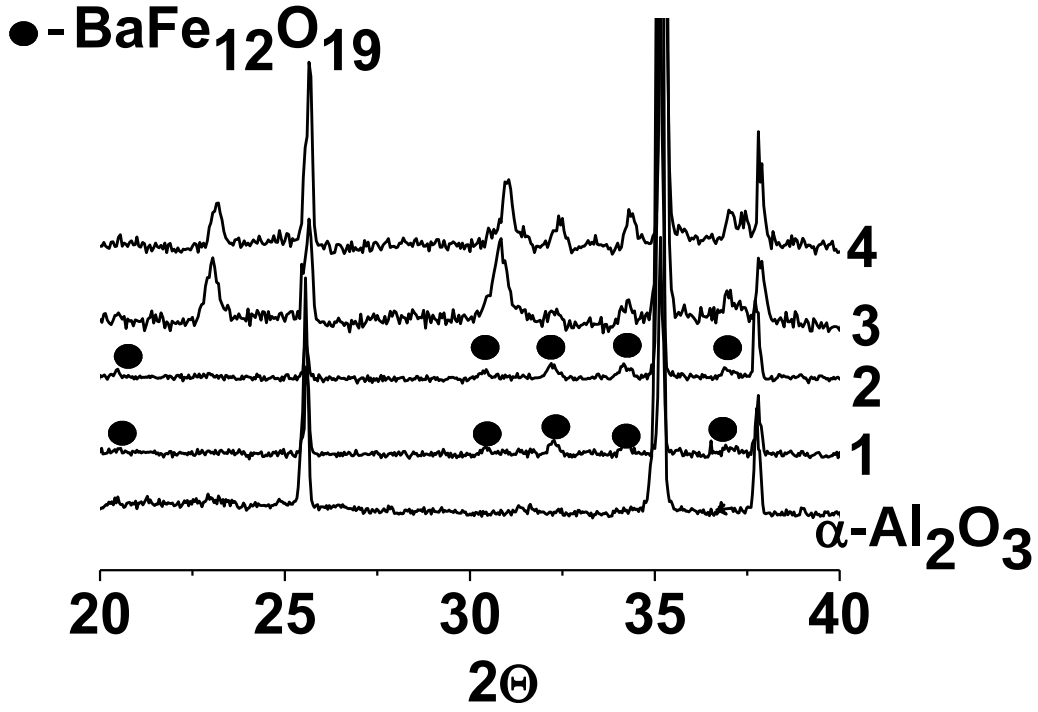

Figure 7

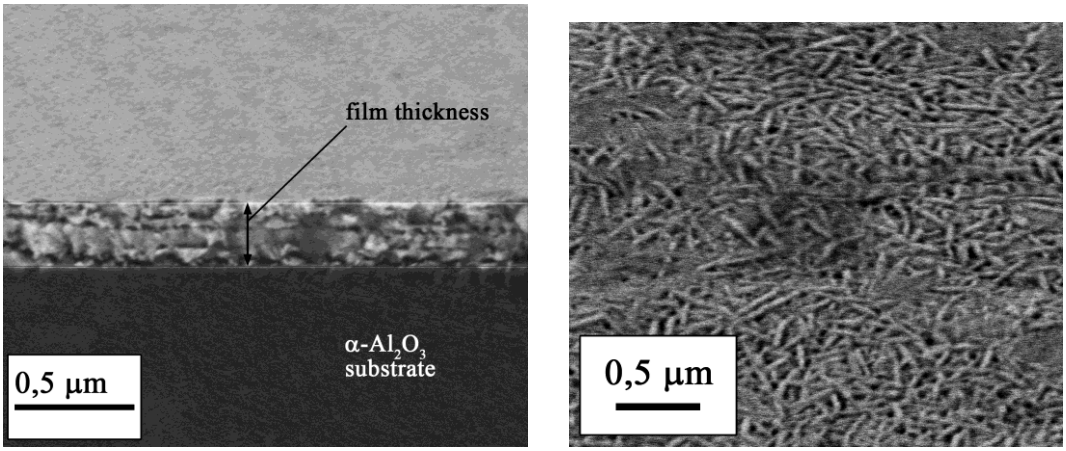

a b

Figure 8

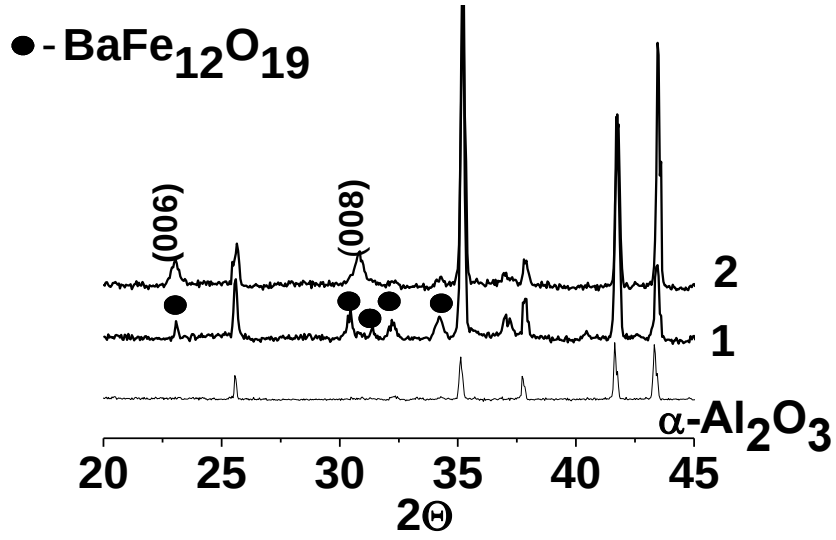

Figure 9

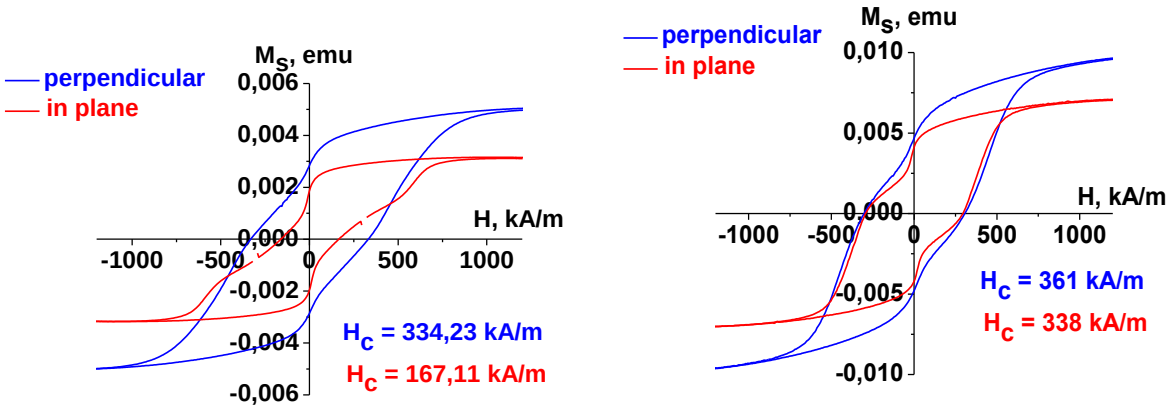
perpendicular
in plane
M_S, emu
0,006
0,004
0,002
0,000
-0,002
-0,004
-0,006
H, kA/m
-1000
-500
0
500
1000
H_C = 334,23 kA/m
H_C = 167,11 kA/m
perpendicular
in plane
M_S, emu
0,010
0,005
0,000
-0,005
-0,010
H, kA/m
-1000
-500
0
500
1000
H_C = 361 kA/m
H_C = 338 kA/m

a b

Figure 10